Single-impurity tunneling spectroscopy to probe the discrete states of a two-dimensional electron gas in a quantizing magnetic field

B. Jouault
Groupe d'Étude des Semiconducteurs, Université Montpellier II, Place E. Bataillon, 34095 Montpellier, France

M. Gryglas, G. Faini, U. Gennser, and A. Cavanna
Laboratoire de Photonique et Nanostructures, Centre National de la Recherche Scientifique, Route de Nozay, 91460 Marcoussis, France

M. Baj
Institute of Experimental Physics, Warsaw University, Hoza 69, 00-681 Warsaw, Poland

D. K. Maude
Grenoble High Magnetic Field Laboratory, Centre National de la Recherche Scientifique, 25 Avenue des Martyrs, 38042 Grenoble, France

(Received 24 November 2005; revised manuscript received 8 March 2006; published 13 April 2006)

A single impurity is used to probe the local density of states of a two-dimensional electron gas (2DEG) in a resonant tunneling experiment. The studies have been performed in the GaAs/AlAs/GaAs system, with Si donors incorporated into the AlAs layer, on submicrometer junctions. The current-voltage characteristics clearly show peaks corresponding to the formation of Landau levels. Moreover, additional fine-structure superimposed on the Landau levels are resolved. Detailed magnetic field studies suggest that those peaks reflect the single particle states of the Landau levels. The surprisingly rapid shift of these additional features in a magnetic field is reproduced in a model, which takes into account disorder in the plane of the 2DEG.

DOI: 10.1103/PhysRevB.73.155415 PACS number(s): 73.43.−f, 73.23.Hk

I. INTRODUCTION

Soon after the discovery of the integer quantum Hall effect in a two-dimensional electron gas, it was realized that plateaus in the Hall resistance would not be observed in the absence of some degree of imperfection and disorder.[1] In a strong magnetic field (B), the magnetic field length, $\ell_B = \sqrt{\hbar/eB}$, becomes smaller than the typical length scale of the disorder potential and the electrons move along equipotential lines, forming single-particle states with discrete energies. The observation of these single-particle states is very delicate. One of the issues is that in a 2DEG, in the presence of a quantizing magnetic field, flat and compressible regions are formed at the Fermi energy ε_F.[2] These regions contain many single-particle states that cannot be observed separately by linear transport measurements. Another issue is the Coulomb blockade effect; in 2DEG's and in large quantum dots, the charging energy usually dominates over the excitation energy.[3–6]

In this paper, we present results obtained in a GaAs/AlAs tunneling structure, in which the local density of states of a 2DEG is analyzed using a single impurity as a local spectrometer. In such devices, the local density of states can be scanned as a function of energy by measuring the current-voltage $[I(V)]$ characteristic.[7,8] For this reason, these structures are especially attractive for the investigation of the single-particle states. Peaks are observed in the current-voltage characteristics due to the formation of Landau levels (LLs) when a magnetic field is applied perpendicular to the 2DEG plane. In addition, fine structure, in the form of a succession of sharp peaks, is superimposed on the resolved LLs. An analysis of the $I(V)$ tunnel characteristics measured at different magnetic fields shows that these sharp peaks are quasiperiodic in B. Two different processes, possibly responsible for these peaks, are discussed; the charging of the 2DEG by additional electrons, or the quantization of the 2DEG density of states for a constant number of electrons.

Taking into account the charging energy alone does not account for the observed behavior of the sharp peaks. We present a simple model with a constant number of electrons in the 2DEG and no electron-electron interaction, that reproduces qualitatively well the behavior of the additional fine structure. In this model a local potential hill is added in the center of the 2DEG. The presence of such a potential hill can be easily justified by the disorder or by the potential deformations induced by the formation of the compressible regions. On the hill slope the energies of single-particle states increase faster than the energy of the LL when the magnetic field increases. If the spectrometer is located somewhere on the slope of the potential hill, then the shift of the sharp peaks is qualitatively well reproduced. The limits of this simple model are also discussed.

II. SAMPLE DESCRIPTION

Experiments were performed on GaAs/AlAs/GaAs single barrier junctions in which a few impurities, intentionally incorporated in the AlAs layer, are involved in the tunneling process. Samples were grown by molecular beam epitaxy on a (100)-oriented Si-doped n-type GaAs wafer

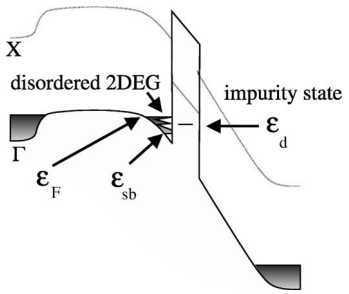

FIG. 1. Schematic of the conduction band structure of the GaAs/AlAs/GaAs tunnel diode under an applied bias. A 2DEG is formed in emitter contact in front of the AlAs barrier. A Si donor intentionally introduced in the barrier scans the local 2DEG density. ε_{sb} is the energy of the lowest subband in the emitter.

($n_d = 1 \times 10^{18}$ cm^{-3}). The active part of the heterostructure consists of a 10.2 nm thick AlAs barrier incorporating a Si δ-doping in the middle with a concentration of $n_\delta = 1 \times 10^{10}$ cm^{-2}. The barrier is separated from the heavily doped contacts ($n_d = 4 \times 10^{18}$ cm^{-3}) by 200 nm thick GaAs spacers. Mesa structures of different lateral sizes ranging from 500 μm down to 100 nm diameter were fabricated. This allows us to have different numbers of donors within the junction, starting from more than 10^6 for the larger mesas down to only a few for the smallest ones.

Figure 1 shows the schematic conduction band structure for our samples. The bands are aligned in such a way that the AlAs layer forms a barrier for the electrons in the Γ valley (black line), and a quantum well for the *X* valley electrons (grey line). Self-consistent solution of the coupled Poisson and Schödinger equations, as well as experiments, show that in our samples the impurity states linked to the *X* valley are aligned with the 2DEG in the emitter when a bias of about 1 V is applied to the device. Hence, the impurities can be used as spectrometers for the 2DEG states. Preliminary results of such a spectroscopy performed on these structures have been published elsewhere.[9]

III. TUNNELING SPECTROSCOPY

Figure 2 presents the $I(V)$ characteristic of a 900 nm mesa measured at very low temperature (20 mK). For such a small mesa the expected number of impurities is estimated to be about 80. For positive bias [Fig. 2(b)], we observe a sharp current increase at 850 mV, which is followed first by a plateau and finally by a decrease of the tunneling current at 950 mV. Such a shape of the tunneling current has been observed in many samples studied, and can be explained in detail.[10] The current increase corresponds to the beginning of the resonant tunneling process via an impurity level, the energy of which becomes aligned with the Fermi energy of the emitter. Then, as the voltage increases further, the energy of impurity level decreases with respect to the Fermi energy, while remaining aligned with occupied states in the 2DEG, so that the tunneling current is maintained. However, for sufficiently large applied biases, the impurity level is pushed below the bottom of the subband in the emitter, and the current decreases. The current does not go to zero exactly because of the importance of inelastic tunneling processes. For negative bias [Fig. 2(a)] an almost identical characteristic is observed, with a current plateau between −850 mV and −950 mV. This shows that the structure is symmetric and that the impurity involved is located close to the center of the barrier. The fluctuations superimposed on the current plateau are not temperature dependent, therefore they do not correspond to other impurities but rather to local density fluctuations of the 2DEG. In the curve presented in Fig. 2, at higher bias, several other current jumps can also be seen. Most of them are due to tunneling via different impurities, however, there are also some indications of tunneling via excited levels of the impurity which participated to the tunneling process at lower bias (850–950 mV). This issue will be discussed in detail elsewhere, and here we will concentrate only on the first observed structure.

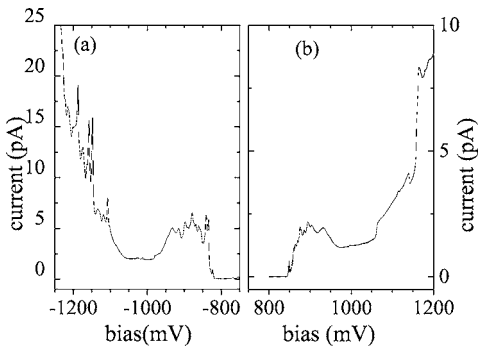

FIG. 2. $I(V)$ curves for positive and negative biases. The first current plateau appears for both polarizations at approximately the same bias voltage of $V \approx \pm 850$ mV.

IV. MAGNETO-TUNNELING SPECTROSCOPY

The application of a quantizing magnetic field further reduces the degrees of freedom of the system and can give valuable additional information concerning the origin and nature of features observed in $I(V)$. Figures 3 and 4 show the $I(V)$ curves in the presence of an applied external magnetic field. The direction of the magnetic field was parallel to the growth direction and the temperature was equal to 20 mK. Figure 3 shows the $I(V)$ curves at different magnetic fields ranging from 0 T (bottom) to 17 T. The magnetic field step is 0.25 T at low fields, 0.5 T for intermediate fields, and 1 T at high fields. Figure 4 shows the curves from 0 T (bottom) to 3.75 T (top). The vertical offset is proportional to the magnetic field. The solid lines are drawn as a guide to the eye to highlight the evolution of the first four spin-degenerate LLs in the 2DEG. The voltage positions of the peaks in $I(V)$ corresponding to the first three LLs are plotted in Fig. 5 as a function B. A linear fit to the LL position has been performed using the expression

$$V_n(B) = V_{sb} - \alpha \hbar \omega_c (n + 1/2) \qquad (1)$$

where n is the LL index, V_{sb} corresponds to the bottom of the electrical subband, α is the leverage factor, $\omega_c = eB/m^*$ is the cyclotron energy, $-e$ is the electron charge, and m^* is the effective mass for GaAs. A least-squares fit (solid

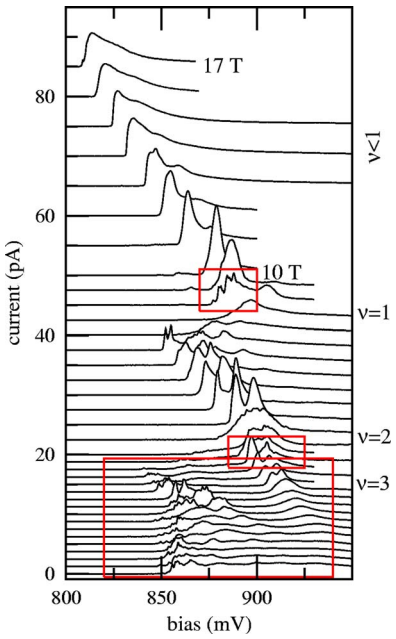

FIG. 3. (Color online) $I(V)$ curves for various values of B ranging from 0 T (bottom) to 17 T (top). For clarity, curves have been offset vertically by an amount proportional to B. The boxed regions, from bottom to top, are presented in detail in Figs. 4, 6, and 8, respectively.

lines) to the data in Fig. 5 gives $\alpha=12.3$ mV/meV and $V_{sb}\approx 946$ mV. By comparison the current threshold (corresponding to the Fermi energy) is found at 855 mV. Knowing the above values, the Fermi energy and the electron

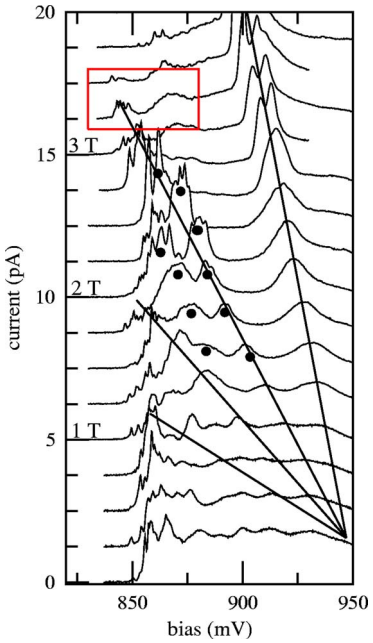

FIG. 4. (Color online) $I(V)$ curves as a function of B for low magnetic fields from 0 T (bottom) to 3.75 T (top). Curves have been shifted for clarity. The boxed area shows the region of fine structure selected for a more detailed presentation in Fig. 7. The closed circles show the splitting of the second LL, which is discussed in Sec. IV E.

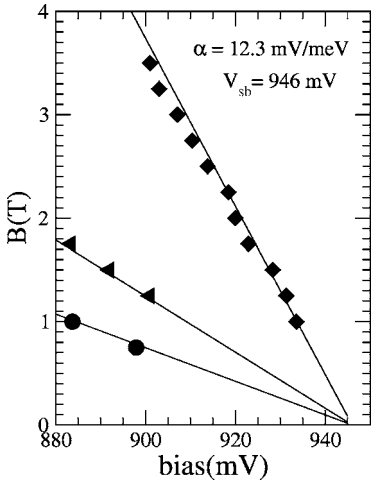

FIG. 5. The positions of the peaks in $I(V)$ measured at different magnetic field corresponding to the LLs $n=0$, 1; and 2 (solid symbols). The solid lines correspond to the best fit as described in the text.

concentration in the emitter were calculated. They equal $\varepsilon_F=7.2$ meV and $n_s=2\times10^{11}$ cm^{-2}, which agrees with the values obtained from the measurements of the macroscopic samples, in which the 2DEG concentration varies from 1.5×10^{11} cm^{-2} to 3×10^{11} cm^{-2} when the bias increases from 500 mV to 1200 mV.[11]

A. Exchange energy and screening

We consider here the evolution of the LL width and shape with magnetic field, in particular we focus on the lifting of the LL spin degeneracy. As usual for a 2DEG in GaAs, the single particle Zeeman energy plays no role (the Landé factor $g^*=-0.44$ for GaAs is too small), while both exchange interaction and screening are important. The exchange interaction is maximum when the Fermi energy lies in a spin gap (when ν is odd); spin splitting is then strongly enhanced. This is clearly seen at high fields ($B\approx 8-9$ T, $\nu=1$), where there is an abrupt change of the lowest LL position which occurs when the LL becomes suddenly spin polarized. Such a sudden polarization has been previously reported in similar devices by another group.[8] In our case, the peak shifts by approximately 41 mV, suggesting a LL splitting of $2\times41/\alpha\approx6.66$ meV. At $B\approx8$ T this corresponds to an effective enhanced g factor of the order of 14. The dependence of screening on filling factor was reported by Ando[12] for the first time. The LL width depends on the position of the Fermi level and becomes very large when the Fermi level lies in the tail of a disorder-broadened LL (i.e., for even ν in the case of spin-degenerate LLs). This is because the disorder cannot be screened efficiently in this case. This effect is perfectly seen in Fig. 3, where there is a sudden and unambiguous increase of the first LL width at $B\approx4-4.5$ T, i.e., close to $\nu=2$, just after the Fermi level emerges out of the second LL. In contrast, we observe a well resolved spin splitting at $\nu\approx3$.

B. Fine structure

Referring to Figs. 3 and 4, one can clearly see that for certain values of the magnetic field, superimposed on the LL

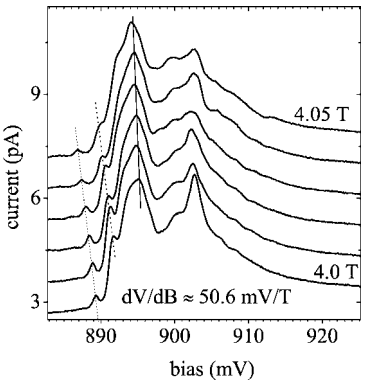

FIG. 6. $I(V)$ obtained for magnetic fields around 4 T. The rather broad main peak corresponds to the first LL. Superimposed on this peak, the fine structure is observed that shifts to a higher energy (lower bias voltage) with B faster than the LL.

peaks, fine structure is observed. These peaks are particularly well resolved when the LL crosses the Fermi energy, see e.g., Fig. 4 at $V \approx 850$ mV, $B \approx 3-3.5$ T and Fig. 3 at $V \approx 900$ mV, $B \approx 9$ T. However, they are also visible when the LL lies below the Fermi energy, as shown in Fig. 6. Such a fine structure has been systematically observed for the large number of samples we have studied.[9,10] Similar fine structure has also been reported in the literature.[8] We also performed experiments with B perpendicular to the current. In such a configuration, neither LLs nor these fine-structure peaks are visible. This is a clear hint that the fine-structure peaks are induced by the formation of the LL. In order to understand their origin, a detailed investigation of their evolution in magnetic field has been performed.

Figure 7(a) shows a gray-scale plot of the current as a function of bias ranging from 830 mV to 880 mV and magnetic field ranging from 3.2 T to 3.65 T, measured at $T=80$ mK. The $I(V)$ curves in Figs. 7 and 4 are not strictly identical because the sample was thermally cycled to room temperature between the two measurements. Here the light areas indicate the highest values of the current. For these voltage and magnetic field conditions, the second LL is visible as a wide light stripe. Its position $V_1(B)$ is marked by the solid line, taken from the observed evolution of the LL in Fig. 5, generated here using Eq. (1). The low energy tail of the LL corresponds to the current valley and is clearly distinguishable around 860–870 mV in Fig. 7(a).

Figure 7(b) presents a cross section of the $I(V,B)$ dependence for a constant field of 3.3 T. There are several fine-structure peaks resolved within the LL. The average energy separation between them is about 175 μeV. The $I(V,B)$ gray-scale plot allows to follow their evolution. One clearly sees that the fine-structure peaks move at a higher rate than the LL itself, approximately three times faster. This difference is too large to be explained by variations of the leverage factor α. Moreover, it is interesting to note that the peaks appear to be quasiperiodic with the magnetic field. This is shown in Fig. 7(c), which presents a cross section for a constant bias $V=846$ mV. The magnetic field period is approximately 20–30 mT. The fast Fourier transform of this $I(B)$ curve is shown in Fig. 7(d). The clear peak appearing at

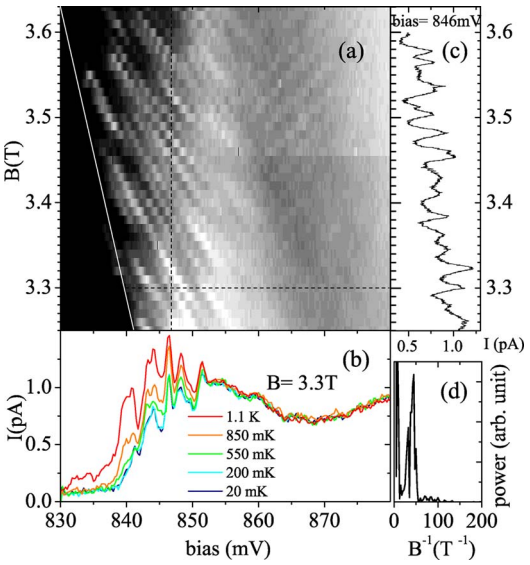

FIG. 7. (Color online) (a) Gray-scale plot of $I(V,B)$ for magnetic fields for which the second LL (large peak between 840 and 860 mV) crosses the Fermi energy. Superimposed on this peak, the fine structure is observed that shifts to a higher energy (lower bias voltage) with B faster than the LL. White solid line: fit of the LL shift from Fig. 5. (b) Temperature dependence of the $I(V)$ curve for $B=3.3$ T (indicated by a dashed line). The increase of the peak height with T is a signature of phonon-assisted tunneling from the localized states of the 2DEG to the single impurity spectrometer. (c) $I(B)$ for a given bias ($U=846$ mV). Peaks have a periodicity of 20–30 mT [the fast Fourier transform of this curve is shown in the bottom-right panel (d)].

30–50 T^{-1} gives further evidence for this periodicity.

In order to explain the origin of the fine structure, a number of hypotheses have to be considered: (i) the peaks can result from the charging of the 2DEG with subsequent electrons; (ii) they can reflect the single particle spectrum in the electron gas; (iii) finally, one could imagine that both effects take place. Let us discuss these issues, starting from the first one. In the nonlinear transport through a confined 2DEG, the effect of charging is well known (Coulomb blockade). Charging becomes important when the electron gas is decoupled from the leads. The 2DEG in question is on one side confined by the AlAs barrier, however, it is not *a priori* evident that there is a barrier on the spacer side. Self-consistent calculations of the potential profile and capacitance measurements of large mesas in magnetic fields suggest that there is a small potential hill between the heavily doped contact and the quantum well. In this case, the charging effect can, in principle, be important. An estimation of the charging energy for a 2DEG in the 900 nm mesas gives about 300 μeV.[13] This value is in a good agreement with the observed separation between the peaks. However, we have observed similar peaks with approximately the same small spacing in much smaller pillars, where the charging energy is expected to be significantly higher.

Charging alone is unable to account for the behavior of the peaks in magnetic field. As pointed out by Bird *et al.*,[4] at a constant bias, whether the number of electrons increases or decreases, depends on what the energy of single-particle

states at ε_F does with increasing B. If the energy of these single-particle states decreases with increasing B, the number of electrons increases and vice versa. In Fig. 7, the second LL is almost empty (it disappears at 3.75 T), indicating that ε_F is pinned by the LL bulk rather than by edge states. Under these conditions, the energy of the single-particle states most probably follows the energy $\approx 3\hbar eB/2m^*$ of the second LL and increases with B, therefore the number of electrons in the second LL decreases when B increases; this corresponds to the case $B>6$ T of Ref. 4.

From another point of view, common sense indicates that at constant magnetic field, the number of electrons can only increase when the bias increases. This is also confirmed by measurements of Shubnikov de Haas oscillations in large mesas, from which it is possible to extract the electron density n_s at different biases. The two observations, that the number of electrons increases when the magnetic field is decreased and when bias is increased, imply that fine-structure peaks resulting from the charging of the LL should shift more slowly than the LL. On the contrary, we observe the opposite trend, with the fine-structure peaks shifting much faster than the LL. One should also keep in mind that at $B\approx 3$ T, two compressible regions, corresponding to the two higher spin-degenerate LLs, may exist. As the magnetic field is increased, a discrete charge $-e$ moves from the inner to the outer compressible region. The renormalization of the potential after the electron transfer should induce current oscillations. As in the previous case, the number of electrons in the inner compressible region (the second LL) decreases when B increases and to first approximation, the fine-structure should shift more slowly than the LL in the (V,B) plane.

Finally, a further reason which suggests the irrelevance of the charging of the 2DEG, is the progressive smoothing of the current fluctuations when they move away from the current threshold. Indeed, the peaks in a Coulomb blockade regime are not smeared out when the number of electrons in the quantum dot increases. In contrast, a smearing of the peaks is a typical signature of a decrease of the quasiparticle lifetime below the Fermi energy.[14,15]

We will now show that taking into account the single particle spectrum alone, but with smooth variations of the potential induced by some disorder, is enough to reproduce the qualitative behavior of the fine-structure peaks. Since the spectrometer is well localized in space, one can associate to it an equipotential line that passes through the position of the single impurity spectrometer and that encloses a region of finite size S. Due to the disorder, this region corresponds to either a hill or a valley of the in-plane slowly varying potential. In the smooth potential approximation,[1] each quantum state occupies the same area $2\pi l_B^2=\Phi_0/B$ and the number of states per LL in this region is BS/Φ_0. When B increases, this number must increase: the states get closer while additional SP states cross regularly at the equipotential line at the edge. By doing that, the states follow the local slope of the potential. Therefore the energy of the peaks increases with B more quickly than the energy of the LL if the equipotential line encloses a potential hill. On the contrary, the energy of the peaks increases more slowly than the LL energy if the equipotential line encloses a valley. Experimentally, the sharp peaks move faster than the LL, indicating that the equipotential line encloses a potential hill.

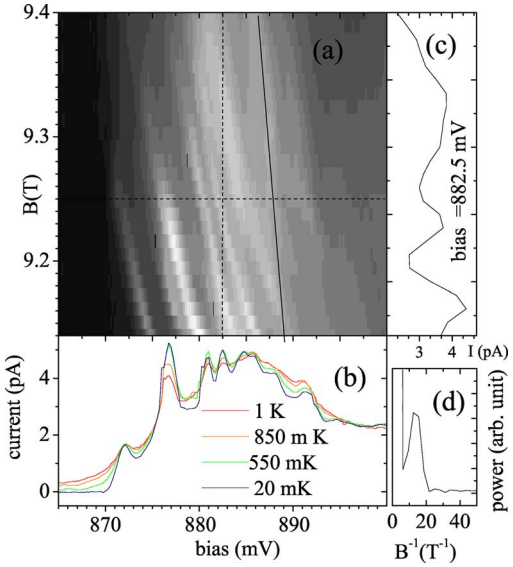

FIG. 8. (Color online) (a) Gray-scale plot of $I(V,B)$, close to the filling factor $\nu=1$. Additional peaks (fine structure) are superimposed on the main peak corresponding to the first spin-split LL. Solid line: expected evolution of the first LL from Fig. 5. Again, the additional peaks (fine structure) shift to higher energy (lower bias voltage) faster than the LL. (b) Temperature dependence of $I(V)$ for $B=9.25$ T. (c) The periodicity [see also the fast Fourier transform in the bottom-right panel (d)] is 2–3 times larger than the periodicity observed for the spin-degenerate second LL in Fig. 7, suggesting that the degeneracy is now given by eB/h.

This interpretation is in agreement with the behavior of the sharp fine-structure peaks at higher B. Figure 8(a) shows a gray-scale plot of the $I(V)$ curves at $\nu\leqslant 1$ (B varies from 9.14 to 9.4 T). This figure is very similar to Fig. 7. The solid line corresponds to the curve $V_0(B)+41$ mV, taken from Eq. (1). The offset of ≈ 41 mV is added to take into account the spin gap. Again, the observed fine structure moves faster than the LL itself. The right panel [Fig. 8(c)] shows an $I(B)$ curve at constant bias from which it is possible to extract a B periodicity (65–100 mT), roughly 2–3 times larger than the B periodicity of 20–30 mT observed at $\nu\approx 2.5$ in Fig. 7. In this magnetic field region there is not a sufficient number of peaks to allow a precise estimate of the period. However, the observed approximate doubling of the period can be explained by the lifting of the spin degeneracy at high B. In this case, when the LL degeneracy is only eB/h, the B periodicity of the sharp peaks should be two times larger. This explanation is valid only if there is a small spin splitting at $B\approx 3.5$ T in the second LL. Such a splitting may be induced either by an additional Coulomb interaction, or by Zeeman effect. For instance, at this magnetic field, the Zeeman spin splitting is of the order of 80 μeV and may be experimentally resolved.

C. Temperature dependence

Another interesting property of the fine-structure peaks is that they have a very strong temperature dependence, as

shown in Fig. 7(b). When the temperature is increased from 20 mK to 1.2 K, the width and height of the current peaks increase monotonically, while their positions remain unchanged. Such a behavior has been reported for phonon-assisted Coulomb blockade oscillations in disordered wires,[16,17] and for phonon-assisted tunneling through an impurity.[18] Following the last reference, and our own previous analysis,[10] we ascribe the increase of the peak height with T to phonon-assisted tunneling from the localized states of the 2DEG to the spectrometer single impurity state. The peak height and width may be calculated using the description of hopping conduction of Shklovskii and Efros.[19] A linear increase of the peak height with the temperature is then expected, as observed experimentally in Fig. 7(b) for temperatures higher than 500 mK. We observe no temperature dependence between 20 mK and 200 mK, probably because at these very low temperatures, in our small mesoscopic devices, the electrons in the 2DEG are not efficiently thermalized.

A rather different temperature dependence is observed in the vicinity of $\nu=1$, where the peaks are simply smeared out when the temperature increases. Figure 8(b) shows the evolution of the fine-structure peaks at $\nu=1$ between 20 mK and 1 K. Above 2 K, all peaks observed in Figs. 7 and 8 are washed out, as expected when the energy ΔE of the excitation becomes comparable to $k_B T$.

D. First estimations

From our simple model, the data shown in Fig. 7, allows us to extract many parameters of the investigated system. The periodicity of the fine-structure peaks ΔB observed at constant bias, around a constant magnetic field B_0, is given by

$$\Delta B = \frac{\Delta E}{\hbar\left(n+\frac{1}{2}\right)\frac{e}{m^*}+\frac{2S}{\Phi_0}\Delta E}, \tag{2}$$

where S is the surface enclosed by the equipotential line passing through the position of the single impurity spectrometer, ΔE is the energy spacing between two consecutive fine-structure peaks observed at constant magnetic field. This formula takes into account the LL shift. Neglecting this shift would lead to the usual formula $\Delta B=\Phi_0/2S$, where the factor 2 arises from the spin splitting. For the sake of simplicity, we assume a circular equipotential line of radius $r_s=\sqrt{S/\pi}$.

From Fig. 7 we estimate $\Delta B \approx 25\pm5$ mT and $\Delta E \approx 175\pm25$ μeV. This gives $r_s=100-150$ nm, consistent with the diameter of the pillar, which is much larger. For a given magnetic field B_0, the in-plane electric field $\mathcal{E}$ is given by

$$e\mathcal{E} = \Delta E \frac{4\pi r_s B_0}{\Phi_0} \tag{3}$$

so that $\mathcal{E}\approx(2.3\pm0.4)\times10^5$ V/m. A similar value is found for $\nu=1$, $\mathcal{E}\approx(2.7\pm0.4)\times10^5$ V/m. In the literature, the reported values of the local electric field in similar systems range from 2×10^4 V/m to 3×10^5 V/m.[20–22] Davies and Nixon[23] calculated the effect of the random placement of impurities in the doped layer of a heterojunction and they found potential fluctuations on a typical length scale of 0.1 μm, of the same order as r_s. They also found local electric fields of $\sim10^5$ V/m, however, they did not take into account the screening by the electrons in the 2DEG that should smooth out the fluctuations. Another probable origin of the high electric fields is the formation of alternating regions of compressible and incompressible liquids in the 2DEG when a magnetic field is applied.[2] This increases dramatically the electric field in the incompressible regions, where the electrostatic potential changes abruptly by $\sim\hbar\omega_c$.

E. A qualitative model

In order to verify the hypothesis that the observed fine-structures reflect the single-particle states in the LLs, a calculation of the resonant tunnel current has been performed. Our simple model assumes that the 2DEG in the pillar is confined by a weak parabolic potential,

$$v_0(r) = \tfrac{1}{2}m^*\omega_d^2 r^2, \tag{4}$$

where ω_d is the strength of the confinement potential, m^* is the effective mass in GaAs, r is the in-plane radius. Such a parabolic potential is realistic for small pillars[24] and has the advantage that the lateral wave functions and eigenvalues are well known.[25]

To reproduce the fine-structure shift, an additional hill of potential $v_1(r)$ is added (see Fig. 9). As a model, we take

$$v_1(r) = v\frac{1}{1+\exp(4e(r-r_s)\mathcal{E}/v)}, \tag{5}$$

where $\mathcal{E}$, r_s, and v are parameters. As defined before, r_s is the position of the single impurity spectrometer (and therefore radius of the potential hill), while $\partial v_1/\partial r(r_s)=e\mathcal{E}$ is the electric field at $r=r_s$ (we have neglected the contribution of the v_0 potential for simplicity). The parameter v controls the

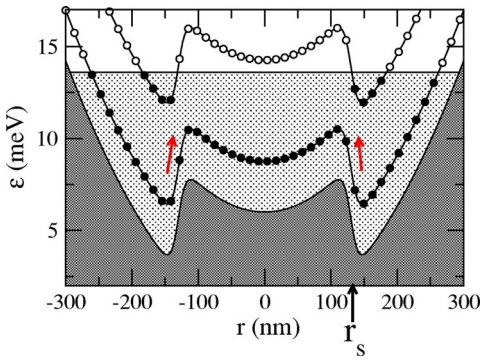

FIG. 9. (Color online) Dark grey area: in-plane potential used for the simulation. The spectrometer position r_s is indicated by a black arrow. The light grey region indicates the states populated at $B=3.2$ T, the two first spin-degenerate LL's are indicated by solid lines. Single-particle states are indicated either by open circles (empty states) or by closed circles (occupied states). The gray (red) arrows indicate how the single-particle states move when B increases.

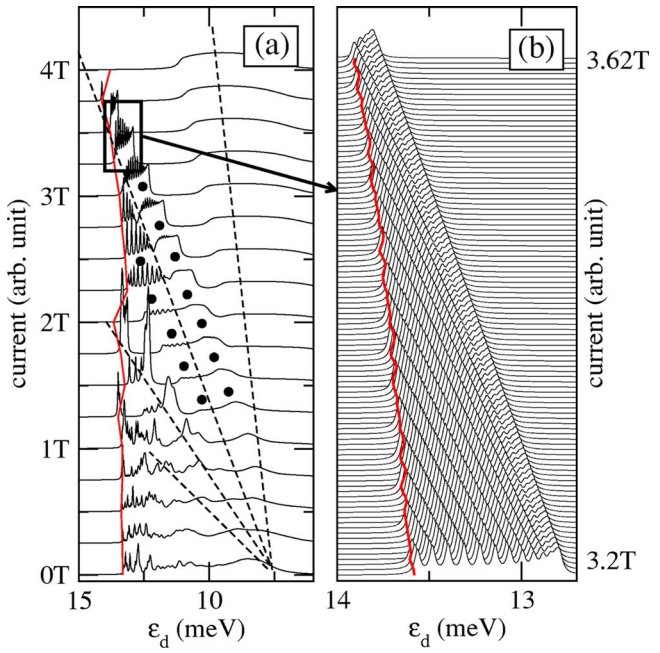

FIG. 10. (Color online) $I(V)$ calculated as described in the text at different magnetic fields. The curves have been vertically shifted for clarity. (a) Magnetic field ranging from 0 T to 4 T; the dashed lines indicate the positions of the LL's. (b) Magnetic fields from 3.2 T to 3.62 T. The gray (red) lines indicate the position of the Fermi level.

overall amplitude of the potential fluctuation.

The eigenvalues ε_i and eigenstates $|i\rangle$ of the total Hamiltonian,

$$H = \frac{(\mathbf{p} + e\mathbf{A})^2}{2m^*} + v_0 + v_1 \tag{6}$$

are calculated as a function of B. The current is proportional to

$$I(\varepsilon_d) \propto \sum_i |\langle r_s|i\rangle|^2 \frac{\Gamma}{(\varepsilon_i - \varepsilon_d)^2 + \Gamma^2} f(\varepsilon_d - \varepsilon_F), \tag{7}$$

where f is the Fermi distribution, ε_d is the spectrometer energy, and we have added a phenomenological broadening parameter Γ that can be divided into two parts: $\Gamma = \Gamma_s + \Gamma_q$, where Γ_s is the spectrometer width and Γ_q corresponds to the decrease of the quasiparticle lifetime far from ε_F. From the experimental data we obtain $\Gamma_s \approx 30$ μeV. For Γ_q we have chosen the usual quadratic dependence,[26] $\Gamma_q = A(\varepsilon_F - \varepsilon_d)^2$, $A = 10$ eV^{-1}, which reproduces the experimental broadening quite well.

Figure 10 shows the results of the simulation, obtained with $\hbar\omega_d = 0.6$ meV, $r_s = 130$ nm, $\mathcal{E} = 2.7 \times 10^5$ V/m, $v = 6$ meV, and $T = 300$ mK. These values have been chosen to be in agreement with the results of the previous section. For our pillar, we estimate that the 2DEG should contain around 200 electrons, in order to obtain the correct Fermi energy of ≈ 7 meV. The introduced potential is shown in Fig. 9. The central depression does not influence the results and could be suppressed by choosing a slightly more complicated trial potential. What is important is the strong local electric field at the position r_s of the spectrometer. A schematic representation of the two first LLs at $B = 3.2$ T is indicated in Fig. 9.

Figure 10(a) shows the calculated $I(V)$ curves from 0 T (bottom) to 4 T (top) with a step of 0.25 T. The main experimental features of Fig. 4, i.e., LLs formation and fine structure, are well reproduced. The first four LLs are indicated by the dashed lines that are drawn as a guide to the eye. They originate from $\varepsilon_d \approx 7.5$ meV at $B = 0$ T, an energy which in first approximation corresponds to $v_0(r_s) + v_1(r_s)$. Figure 10(b) shows the calculated $I(V)$ curves for the second LL only, from 3.2 T to 3.62 T. As observed experimentally in Fig. 7, the fine structure moves significantly faster than the LL itself.

Similar calculations have been performed for the potential v_0 alone (not shown); in this case the equipotential encloses a valley of the potential and, as expected, the opposite trend was found, with the fine-structure peaks shifting more slowly than the LL in a magnetic field.

In addition, our simple model predicts another experimental observation. The second LL, shown in Fig. 4, is composed of two maxima, as indicated by the closed circles. This doublet cannot be due to the spin splitting in GaAs, which is very small for this magnetic field range. This is also confirmed by the fact that the spin splitting observed in the first LL at $B = 3$ T is much smaller than the observed splitting of the second LL, which occurs at $B \approx 1.5$–2.5 T; the double structure of the LL reflects the shape of the wave function of the second LL. The wave functions $|i\rangle$ remain in this aspect similar to the unperturbed wave functions of the second LL, which have a node. When the magnetic field is changed the node moves, and as it crosses the position of the impurity the current decreases. This effect does not occur for the first LL, for which the corresponding wave functions have no node. The simulation reproduces quite well these effects, as shown in Fig. 10(a), where the splitting is also indicated by the closed circles.

It is interesting to note that the calculations also reflect well the experimental $I(V)$ for the case where no magnetic field is applied; fluctuations of the local density of states are resolved. We also stress that the lateral confinement of the pillar plays a minor role in the results at high magnetic fields. In the simulation the current fluctuations are induced by fluctuations of the potential, and not by the lateral confinement. As a last remark, the possible impact of the short range potential centers was evaluated with additional simulations. Several deltalike potentials (≈ 30) were introduced in the 2DEG. It appears that they do not have significant effect on the high magnetic field results without deltalike potentials presented above.

Although many physical observations are properly described with the model proposed, it nevertheless has some limitations. For the parameters used, the energy difference ΔE between the fine-structure peaks is smaller than experimentally observed. Further refining of the parameters is unable to correct this problem. Increasing v simply causes the LLs to disappear. Equally, increasing $\mathcal{E}$ does not work once the wave functions become larger than the potential step. In

order to improve agreement and to obtain a quantitative description, it is probably necessary to take into account the electron-electron interactions. Moreover, the calculations suggest that the fine-structure peaks should also be observed for the first polarized LL. However, this prediction is not confirmed by the experiment; no fine structure is observed above 13 T.

Finally, the large overall amplitude v of the hill potential, associated with the important electric fields close to the edge, suggests that compressible and incompressible regions are formed in the 2DEG. Compressible regions are known to be quite large, while in contrast, incompressible regions are narrow and may induce important fluctuations of the potential. Furthermore, two successive plateaus of compressible region are separated by an energy of the order of $\hbar eB/m^* \approx 6$ meV at $B \approx 3.5$ T, a value compatible with the value of v and our experimental data.

V. CONCLUSION

We stress here that periodic conductance fluctuations have already been observed in devices with two-dimensional dots[3,4,6,27] and antidots.[20,28] These fluctuations were primarily understood as being due to single resonances through single particles states with discrete energies. For dots, it is generally admitted that this explanation is too simplistic; a complete interpretation of these oscillations should take into account Coulomb charging[4] and a correct treatment of the self-consistent potential.[6] For antidots devices, the situation is even more controversial, as it was often assumed that Coulomb blockade effect does not occur in antidots,[20] while recent experiments demonstrate the opposite.[28]

In our case, the vertical transport configuration allows us to investigate the properties of the electron gas not only at the Fermi level, as is the case for standard transport experiments, but also below the Fermi energy. The study of the density of states of the electron gas in magnetic fields reveals, in addition to the formation of the LLs, the existence of a series of fine-structure peaks superimposed on the LLs close to the Fermi energy. A systematic investigation of these peaks shows that they are quasiperiodic in magnetic field. Most of the features observed experimentally can be successfully explained by fluctuations of the potential, in a single particle model. We find no evidence of charging processes. For further investigations, additional magnetotransport measurements on pillars should be performed. Pressure measurements may also give information on the nature of the peaks. The fine structure has been seen in every sample in which the LLs were resolved; two of these samples are presented in Ref. 9; another one in Ref. 10. Results obtained with other samples have never been published but showed LLs with well resolved fine-structure peaks. We have analyzed the shift of the fine-structure peaks for the two samples for which we have a sufficiently complete data set. One of these samples is presented in this paper, while in the other one, we could not clearly differentiate the rate of the fine-structure peaks and the rate of the LLs. In our model, the faster or slower shift of the fine-structure peaks with respect to the LL, is in some sense accidental, since it depends on the position of the single impurity spectrometer, which can be either on a potential hill or in a potential valley. If the potential fluctuations are really random, in some pillars it should be possible to observe a slower shift of the fine structure under a magnetic field.

ACKNOWLEDGMENTS

This work was supported by the European Associated Laboratory "NODLab." Financial support by the Conseil Général de l'Essonne is gratefully acknowledged. Access to the Grenoble High Magnetic Field Laboratory is provided through European Community Contract No. RITA-CT-2003-505474.

[1] *The Quantum Hall Effect*, edited by R. E. Prange and S. M. Girvin (Springer-Verlag, New York, 1987).

[2] C. W. J. Beenakker, Phys. Rev. B **44**, 1646 (1991); Phys. Rev. Lett. **64**, 216 (1990); D. B. Chklovskii, B. I. Shklovskii, and L. I. Glazman, Phys. Rev. B **46**, 4026 (1992).

[3] B. W. Alphenaar, A. A. M. Staring, H. van Houten, M. A. A. Mabesoone, O. J. A. Buyk, and C. T. Foxon, Phys. Rev. B **46**, 7236 (1992).

[4] J. P. Bird, K. Ishibashi, M. Stopa, Y. Aoyagi, and T. Sugano, Phys. Rev. B **50**, 14983 (1994).

[5] J. P. Bird, K. Ishibashi, Y. Aoyagi, and T. Sugano, Phys. Rev. B **53**, 3642 (1996).

[6] P. L. McEuen, E. B. Foxman, Jari Kinaret, U. Meirav, M. A. Kastner, Ned S. Wingreen, and S. J. Wind, Phys. Rev. B **45**, 11419 (1992).

[7] T. Schmidt, R. J. Haug, V. I. Falko, K. v. Klitzing, A. Forster, and H. Luth, Phys. Rev. Lett. **78**, 1540 (1997).

[8] P. C. Main, A. Thornton, R. J. A. Hill, S. T. Stoddart, T. Ihn, L. Eaves, K. A. Benedict, and M. Henini, Phys. Rev. Lett. **84**, 729 (2000).

[9] M. Gryglas, M. Baj, B. Jouault, A. Raymond, C. Chaubet, B. Chenaud, J. L. Robert, and G. Faini, Int. J. Nanosci. **2**, 585 (2003).

[10] M. Gryglas, M. Baj, B. Chenaud, B. Jouault, A. Cavanna, and G. Faini, Phys. Rev. B **69**, 165302 (2004).

[11] M. Gryglas, Ph.D. thesis, Warsaw University, Warsaw, 2004.

[12] T. Ando, J. Phys. Soc. Jpn. **43**, 1616 (1977).

[13] This is the charging energy e^2/C with C being the capacitance of two flat capacitors connected in parallel, both having the surface of the mesa, the same thickness of 200 nm, and a relative dielectric constant of 10.

[14] J. P. Holder, A. K. Savchenko, V. I. Fal'ko, B. Jouault, G. Faini, F. Laruelle, and E. Bedel, Phys. Rev. Lett. **84**, 1563 (2000).

[15] T. Schmidt, R. J. Haug, V. I. Fal'ko, K. v. Klitzing, A. Förster, and H. Lüth, Europhys. Lett. **36**, 61 (1996); J. Könemann, P. König, T. Schmidt, E. McCann, Vladimir I. Fal'ko, and R. J.

Haug, Phys. Rev. B **64**, 155314 (2001).
[16] A. A. M. Staring, H. van Houten, C. W. J. Beenakker, and C. T. Foxon, Phys. Rev. B **45**, 9222 (1992).
[17] J. Wróbel, T. Dietl, K. Regiński, and M. Bugajski, Phys. Rev. B **58**, 16252 (1998).
[18] A. K. Savchenko, V. V. Kuznetsov, A. Woolfe, D. R. Mace, M. Pepper, D. A. Ritchie, and G. A. C. Jones, Phys. Rev. B **52**, R17021 (1995).
[19] B. I. Shklovskii and A. L. Efros, *Electronic Properties of Doped Semiconductors, Solid State Sciences* (Springer-Verlag, Berlin, 1984), Vol. 45.
[20] I. J. Maasilta and V. J. Goldman, Phys. Rev. B **57**, R4273 (1998).
[21] J. A. Simmons, H. P. Wei, L. W. Engel, D. C. Tsui, and M. Shayegan, Phys. Rev. Lett. **63**, 1731 (1989).
[22] P. A. Lee, Phys. Rev. Lett. **65**, 2206 (1990).
[23] J. H. Davies and J. A. Nixon, Phys. Rev. B **39**, 3423 (1989).
[24] A. Kumar, S. E. Laux, and F. Stern, Phys. Rev. B **42**, 5166 (1990).
[25] V. Fock, Z. Phys. **47**, 446 (1928).
[26] D. Pines and P. Nozieres, *The Theory of Quantum Liquids* (Benjamin, Washington, 1966).
[27] B. J. van Wees, L. P. Kouwenhoven, C. J. P. M. Harmans, J. G. Williamson, C. E. Timmering, M. E. I. Broekaart, C. T. Foxon, and J. J. Harris, Phys. Rev. Lett. **62**, 2523 (1989).
[28] M. Kataoka, C. J. B. Ford, G. Faini, D. Mailly, M. Y. Simmons, and D. A. Ritchie, Phys. Rev. B **62**, R4817 (2000); M. Kataoka, C. J. B. Ford, G. Faini, D. Mailly, M. Y. Simmons, D. R. Mace, C.-T. Liang, and D. A. Ritchie, Phys. Rev. Lett. **83**, 160 (1999).